Scanning Electrochemical Microscopy. 55. Fabrication and Characterization of Micropipet Probes

Darren A. Walsh, José L. Fernández, Janine Mauzeroll,[†] and Allen J. Bard*

Department of Chemistry and Biochemistry, University of Texas at Austin, Austin, Texas 78712

The fabrication and characterization of novel micropipet probes for use in scanning electrochemical microscopy (SECM) are described. These can be used to dispense small (pL) amounts of a solution while monitoring the electrochemical response at a substrate and at a ring electrode tip on the micropipet probe. The probes were constructed by insulating gold-coated borosilicate micropipets with electrophoretic paint and exposing a ring electrode at the tip by heat treatment. Characterization of the probes was performed using scanning electron microscopy, cyclic voltammetry, and SECM approach curve experiments. Routine construction of tips with diameters of the order of 3 μm was possible using this technique. The probes exhibited stable steady-state currents and positive and negative feedback approach curves that agreed with those predicted by theory. Demonstrative SECM imaging experiments were performed using a picodispenser to continuously dispense an electroactive solution (ferrocenemethanol) to the SECM cell while the probe was located within a few micrometers of a Pt substrate surface. Oxidation of the dispensed electroactive solution was performed at the substrate, and feedback currents were measured at the probe tip by holding the gold ring at a reducing potential. This mode of tip-dispensing SECM was used to obtain images of a platinum substrate electrode while monitoring both the substrate current and the feedback current at the probe.

Since the development of scanning electrochemical microscopy (SECM), the most widely used modes have been the feedback and generation−collection modes employing solid, disk-shaped ultramicroelectrodes (UMEs).[1,2] However, in recent years, a number of groups have begun to develop novel hybrid SECM techniques, combining novel instrumentation with new probe designs. For example, SECM has been combined with atomic force microscopy,[3−5] electrochemiluminescent detection,[6] and electrochemical quartz crystal microbalance measurements.[7] Such developments have allowed the application of SECM to an increasingly diverse array of samples and increased the available resolution. A number of papers have described novel SECM probes that deviate completely from the traditional insulated solid electrode design. For example, for the examination of transparent samples, a hybrid SECM/optical microscopy (OM) technique has been described that employed polymer-insulated, metal-coated optical fibers as a light source that allowed current measurement at a ring electrode.[8,9]

We describe here the use of micropipets as SECM probes. Previous reports of micropipet electrodes have focused primarily on their use as ion-selective electrodes in monitoring ion-transfer reactions.[10−13] In addition, enzyme-filled glass pipets have been used as SECM probes to monitor the catalytic activity of electrode surfaces.[14] Scanning chemiluminescence microscopy (SCLM), a technique developed recently by Matsue and co-workers, uses a dispensing micropipet (1−2-μm diameter) probe.[15,16] Combined studies using SECM/SCLM were performed using two different probes, a pipet and a UME, suggesting the use of a single dispensing pipet−UME probe, i.e., an amperometric pipet as an SECM probe. Such an SECM tip will allow one to probe numerous applications that are currently beyond the scope of SECM. For example, a useful application will be in novel electrocatalyst screening. The use of tip generation-substrate collection (TG−SC) mode SECM in screening electrocatalysts for O_2 reduction has recently been described.[17] In this method, O_2 was generated at a metal tip, which diffused to a C substrate, upon which multimetallic electrocatalyst mixtures were supported. Monitoring the substrate current then allowed a direct measure of the electrocatalytic activity of the mixtures. However, the major

---

* To whom correspondence should be addressed. E-mail: ajbard@mail.utexas.edu.

† Current address: Laboratoire d'èlectrochimie molèculaire; Universitè Paris 7, Denis Diderot, 2 place Jussieu, 75251 Paris Cedex 05, France.

(1) Bard, A. J. In *Scanning Electrochemical Microscopy*; Bard, A. J., Mirkin, M. V., Eds.; Marcel Dekker: New York, 2001; pp 2−4.
(2) Mirkin, M. V.; Horrocks, B. R. *Anal. Chim. Acta* **2000**, *406*, 119.
(3) Macpherson, J. V.; Unwin, P. R. *Anal. Chem.* **2000**, *72*, 276.
(4) Macpherson, J. V.; Unwin, P. R. *Anal. Chem.* **2001**, *73*, 550.
(5) Kranz, C.; Friedbacher, G.; Mizaikoff, B.; Lugstein, A.; Smoliner, J.; Bertagnolli, E. *Anal. Chem.* **2001**, *73*, 2491.
(6) Fan, F.-R. F.; Cliffel, D.; Bard, A. J. *Anal. Chem.* **1998**, *70*, 2941.
(7) Cliffel, D. E.; Bard, A. J. *Anal. Chem.* **1998**, *70*, 1993.
(8) Lee, Y.; Bard, A. J. *Anal. Chem.* **2002**, *74*, 3626.
(9) Lee, Y.; Ding., Z.; Bard, A. J. *Anal. Chem.* **2002**, *74*, 3634.
(10) Liu, B.; Shao, Y.; Mirkin, M. V. *Anal. Chem.* **2000**, *72*, 510.
(11) Yuan, Y.; Amemiya, S. *Anal. Chem.* **2004**, *76*, 6877.
(12) Shao, Y.; Mirkin, M. V. *Anal. Chem.* **1998**, *70*, 3155.
(13) Amemiya, S.; Bard, A. J. *Anal. Chem.* **2000**, *72*, 4940.
(14) Hengstenberg, A.; Kranz, C.; Schuhmann, W. *Chem. Eur. J.* **2000**, *6*, 1547.
(15) Kasai, S.; Zhao, H.; Matsue, T. *Chem. Lett.* **2000**, 200.
(16) Hirano, Y.; Mitsumori, Y.; Oyamatsu, D.; Nishizawa, M.; Matsue, T. *Biosens. Bioelectron.* **2003**, *18*, 587.
(17) Fernandez, J. L.; Walsh, D. A.; Bard, A. J. *J. Am. Chem. Soc.*, **2005**, *127*, 357.

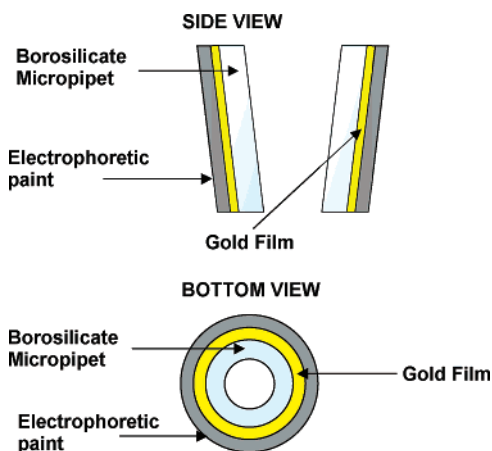**SIDE VIEW**

Borosilicate
Micropipet

Electrophoretic
paint

Gold Film

BOTTOM VIEW

Borosilicate
Micropipet

Gold Film

Electrophoretic
paint

Figure 1. Side- and bottom-view schematics of SECM micropipet probes.

limitation of this screening method (and TG−SC SECM, in general) is that one is limited to species that may be generated electrochemically at the tip. Using pipet probes to dispense solutions, it will be possible to screen electrocatalysts for other reactions, such as methanol or glucose oxidation. These new probes may also prove useful in various biological applications of SECM. For example, it should be possible to dispense drugs to single, immobilized biological cells and electrochemically detect cellular metabolite efflux with high spatial resolution from the cell surface.

The probes described here are based on the design principles used in the construction of SECM/OM probes,[8] and a schematic is shown in Figure 1. Glass micropipets are coated with a thin film of gold. By insulating the sides with an electrophoretic paint and heat curing, it is possible to expose a gold ring electrode located around the pipet aperture. This method of insulation and electrode exposure has proven very effective for the construction of electrodes with submicrometer dimensions.[18−22] A central feature of SECM is the ability to accurately determine the position of a tip relative to the substrate surface (z-displacement) based on the feedback current between the tip and the substrate. The presence of the gold ring around the aperture allows one to control the z-displacement of the probe with nanometer resolution by monitoring the feedback current at the ring electrode.

In this contribution, the construction and characterization of these probes are described. Characterization consisted of SEM analysis, to estimate the quality of the pipet insulation and the diameter of the gold ring electrode. Cyclic voltammetry and SECM approach curves were then used to characterize the geometry of the probe tips. In particular, approach curve experiments can provide a very good insight into the geometry of the probe tips, including the ratio of inner to outer ring diameter and the thickness of the insulating layer, by fitting experimental approach curves to theoretical curves.[23] Finally, a demonstrative SECM

(18) Slevin, C. J.; Gray, N. J.; Macpherson, J. V.; Webb, M. A.; Unwin, P. R. *Electrochem. Commun.* **1999**, *1*, 282.
(19) Conyers, J. L.; White, H. S. *Anal. Chem.* **2000**, *72*, 4441.
(20) Chen, S.; Kucernak, A. *J. Phys. Chem. B* **2002**, *106*, 9396.
(21) Güell, A. G.; Díez-Pérez, I.; Gorostiza, P.; Sanz, F. *Anal. Chem.* **2004**, *76*, 5218.
(22) Watkins, J. J.; Chen, J.; White, H. S.; Abruña, H. D.; Maisonhaute, E.; Amatore, C. *Anal. Chem.* **2003**, *75*, 3962.

imaging experiment is described where a solution of an electro-active species was dispensed from the pipet while scanning the probe across a Pt substrate. Dispensing was performed using a picodispenser that allows one to apply low pressures to the pipet, yielding injected volumes that are a function of the applied pressure and pipet aperture diameter. By holding the substrate at a sufficiently positive potential, it was possible to obtain an image of the Pt substrate by monitoring the substrate oxidation current. Product formed at the substrate electrode diffused back to the probe where it was reduced, allowing us to obtain an image of the substrate by monitoring the feedback current at the tip.

EXPERIMENTAL SECTION

Materials. Borosilicate glass capillaries (length 102 mm/o.d. 1.5 mm/i.d. 1.12 mm) were from World Precision Instruments (Sarasota, FL). Anodic electrophoretic paint (Glassophor ZQ 84-3225) was from BASF (Münster, Germany) and was diluted 1:20 with water prior to use. Silver epoxy was from Epoxy Technology (Billerica, MA). Ferrocenemethanol (Aldrich, Milwaukee, WI) and KCl (Mallinckrodt, Paris, KY) were of reagent grade and used as received. 18 MΩ Ultrapure water (Milli-Q, Millipore Corp., Bedford, MA) was used to prepare all solutions.

Pipet Probe Preparation. Borosilicate glass capillaries were pulled using a filament micropipet puller (model P97, Sutter Instruments, Novato, CA). The shape of the pulled pipet tips depends critically on the parameters used in the pulling step. The pull parameters used in the Sutter Instruments built-in software were as follows (note: these may vary depending on the age of the filament and other unique puller characteristics)

line 1.   heat 590:pull 0:velocity 25:time 250

line 2.   heat 590:pull 0:velocity 25:time 250

line 3.   heat 590:pull 0:velocity 25:time 250

line 4.   heat 500:pull 0:velocity 25:time 250

With these conditions, the total filament heating time during pulling was 14 s. It was possible to form pipets that had tapers that were ∼0.5 cm in length and were symmetrical about the center axis. The aperture sizes obtained using these parameters were reproducible and were of the order of 1.9 μm in diameter.

The ends of the pipets were then coated with gold by vacuum evaporation (Denton Vacuum model DV-502A, Moorestown, NJ) while rotating the pipets at a rate of 30 rpm. After cooling, electrical contact was made to the gold-coated pipets using copper wire with silver epoxy and heat curing at 100 °C overnight. Gold ring electrodes were prepared by insulation of the gold-coated pipets using anodic electrophoretic paint with subsequent exposure of the tip, exposing the ring electrode. Prior to immersion of a pipet into the paint solution, the top was connected to a nitrogen source and nitrogen was passed through the pipet at a pressure of ∼70 psi during the entire deposition step. This prevented clogging of the aperture by particulate material from the paint solution. The end of the pipet was then immersed in electrophoretic paint solution to a depth of ∼0.75 cm. A Pt coil counter electrode (∼1-cm diameter) surrounded the immersed pipet, maintaining

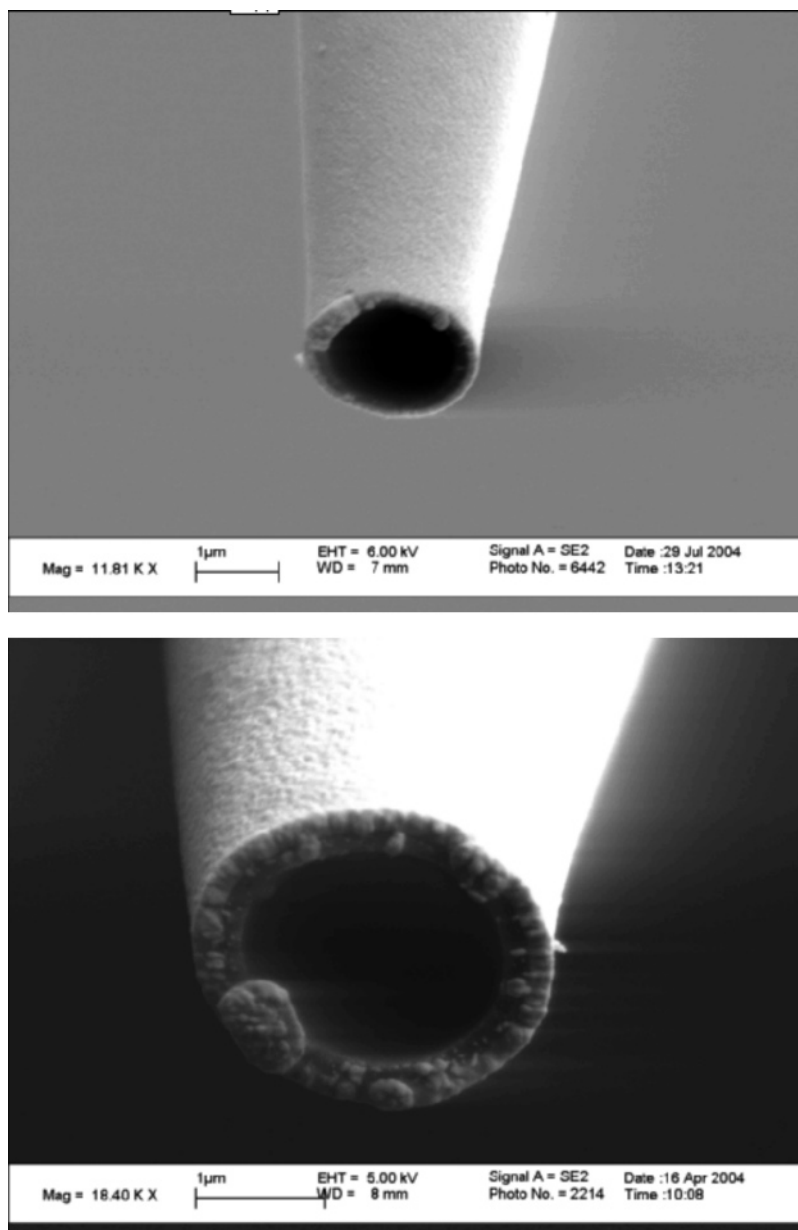(23) Lee, Y.; Amemiya, S.; Bard, A. J. *Anal. Chem.* **2001**, *73*, 2261.

Figure 2. SEM images of gold-coated, borosilicate micropipets prior to insulation.

the pipet at the center of the coil. A constant potential of 2.2 V was then applied between the gold-coated pipet and the platinum counter electrode with a model CHI 660 potentiostat (CH Instruments, Austin, TX) until the current decreased to a small, steady-state value (~30 s). After deposition, the pipet was rinsed with water, the nitrogen source was removed, and the tip was heated at 150 °C for 3 min with the tip pointing upward (perpendicular to the plane of the laboratory floor). An identical, second electrophoretic paint deposition step (including passage of nitrogen through the tip when in contact with paint solution and heat treatment) was carried out to ensure complete insulation of the sides of the pipet.

Electrochemical and SECM Measurements. Initial electrochemical measurements were performed using a standard three-electrode system. The pipet probe was the working electrode, and the counter and reference electrodes were a platinum wire and a Ag/AgCl electrode, respectively. A CH Instruments model CHI

900B (SECM) was employed for electrochemical and SECM measurements. A 2-mm-diameter Pt disk was used as the substrate electrode. Tip dispensing experiments were carried out using a model PLI-100 Pico-Injector (Harvard Apparatus, Holliston, MA).

RESULTS AND DISCUSSION

Scanning Electron Microscopy. Figure 2 shows typical gold-coated pulled glass pipets obtained after vacuum evaporation of gold metal. These images allow an estimation of the diameter of the pipet aperture (nominally 1.9 μm), as well as the thickness of the deposited gold layer (nominally 200 nm). The estimated outer diameter of the gold ring electrode is 2.6 μm. Figure 3 shows typical images of pipets that had been insulated using electrophoretic paint. The thickness of the body of the pipet tip clearly increases upon insulation while the gold ring appears to remain exposed after heat treatment. These images do not yield a clear
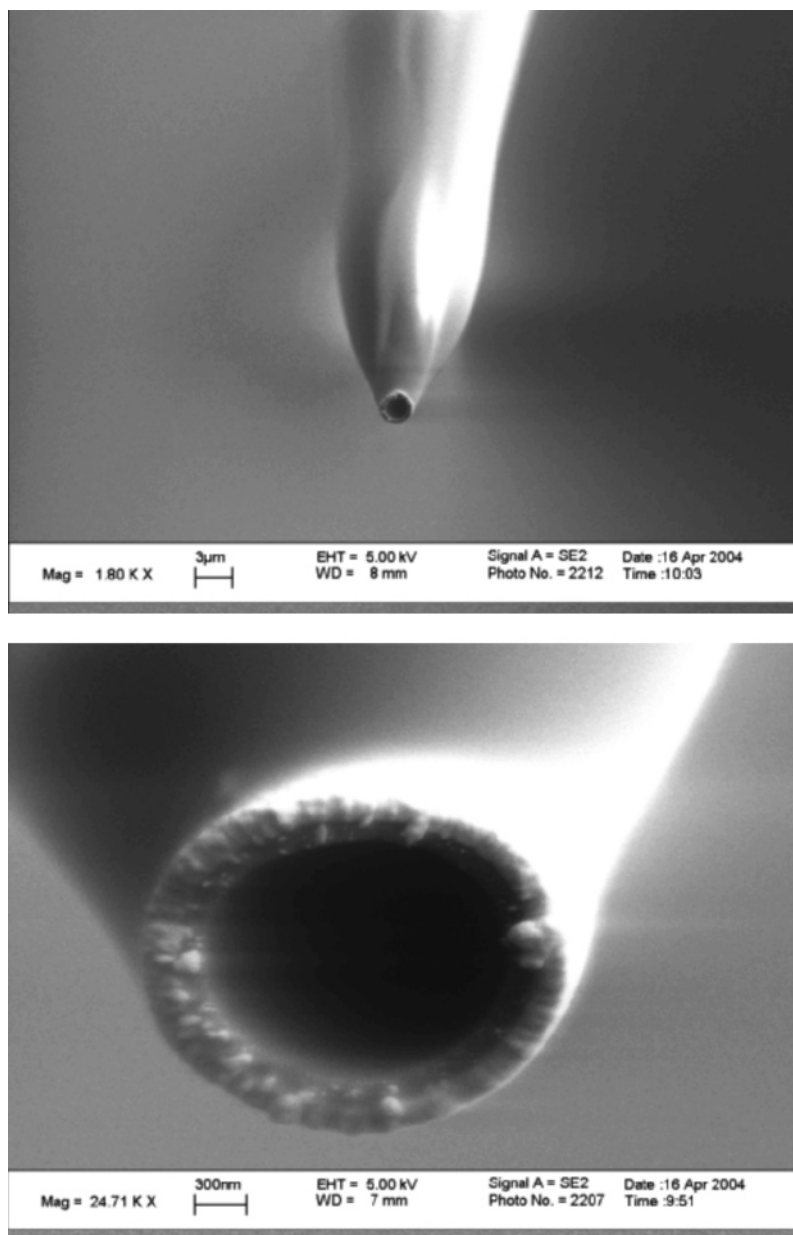
Figure 3. SEM images of gold-coated, borosilicate micropipets after insulation with electrophoretic paint.

estimate of the thickness of the insulating layer surrounding the gold electrode. However, this information can be obtained from analysis of approach curve experiments, and this is discussed in a later section. In addition, electrochemical measurements on these probes can allow one to compare the estimated ring geometry (from scanning electron microscopy, SEM) with that determined electrochemically.

Electrochemical Characterization of Pipet SECM Probes. After SEM analysis of the SECM pipet probes, electrochemical characterization was necessary to ensure that a good insulating layer had been deposited on the exterior and that the gold ring electrode had been exposed completely during the heating step. To verify complete insulation, approach curve experiments were performed by translating the insulated pipet from air into a solution containing a redox-active species. The potential of the pipet electrode was held at a −0.35 V versus Ag/AgCl to reduce $Ru(NH_3)_6^{3+}$ in solution, and the tip current was monitored as the

tip entered the solution from air. A typical approach curve from air for a pipet that exhibits a good insulating layer is shown in Figure 4A. As the probe approached from air, zero current flowed at the probe. When the probe entered the solution, a current began to flow at the probe as the gold ring electrode contacted the solution and $Ru(NH_3)_6^{3+}$ was reduced. As the probe was immersed deeper into the solution, the current did not increase, indicating that a fully insulating layer had been deposited on the electrode. Figure 4B shows the response obtained for a pipet that was not fully insulated. As the probe was immersed deeper into the solution after the initial contact of the ring electrode, a series of current increases was observed. Each of these current increases is caused by the presence of pinholes in the insulating layer on the pipet probe, which contacted the solution as the probe was immersed deeper into the solution.

Once it had been confirmed that a fully insulated pipet probe had been constructed, cyclic voltammetry and SECM approach
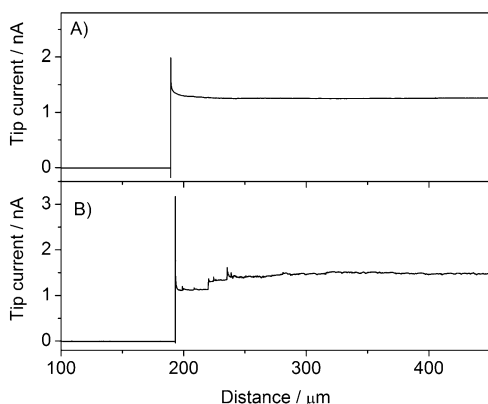
Figure 4. (A) Air to liquid approach curve for an insulated pipet exhibiting a good insulation layer. The potential of the working electrode is −0.35 V vs Ag/AgCl, and the solution contains 4.7 mM ruthenium hexamine chloride with 0.5 M KCl as supporting electrolyte. (B) Air to liquid approach curve for a pipet exhibiting a poor insulating film. Conditions are as in (A).
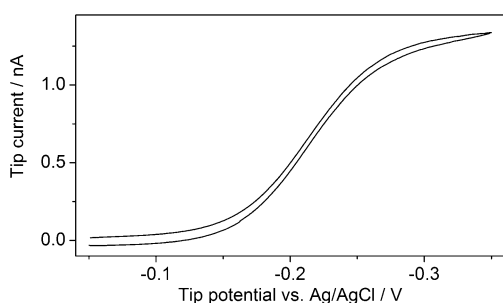

Figure 5. Cyclic voltammogram for a fully insulated SECM pipet in a solution containing 4.7 mM $Ru(NH_3)_6^{3+}$ and 0.5 M KCl as supporting electrolyte. The potential limits were −0.05 to −0.35 V vs Ag/AgCl, and the initial potential was −0.05 V vs Ag/AgCl. The sweep rate was 20 mV s^{-1}.

curve experiments were performed to characterize the pipet ring electrode. A cyclic voltammogram obtained at an exposed ring electrode in 4.7 mM $Ru(NH_3)_6^{3+}$ solution is shown in Figure 5. The shape of the voltammogram agrees with that expected for a freely diffusing species at a microelectrode surface,[24] indicating successful exposure of the gold microring. An approach for estimating the dimensions of ring microelectrodes from steady-state cyclic voltammetry data has been reported,[23] in which the ratio of the steady-state currents obtained at disk electrodes to those obtained at ring electrodes with similar radii was reported for a range of dimensions. For the electrodes described here, the ratio of the inner (a) to the outer (b) radii of the ring is ∼0.8. Using this approach, we can determine that the ring electrode will produce a steady-state current that is 12% lower than that obtained at a disk electrode with a radius b. Therefore, the steady-state current measured at the ring electrode, 1.35 nA, corresponds to a calculated disk current of 1.51 nA. The current at a disk electrode is given by

$$i_{T,\infty} = 4nFDC_0b \qquad (1)$$

where F is the Faraday constant (96 485 C mol^{-1}), D is the

(24) Bard, A. J.; Faulkner, L. R. *Electrochemical Methods: Fundamentals and Applications*; Wiley: New York, 2001; pp 232−233.
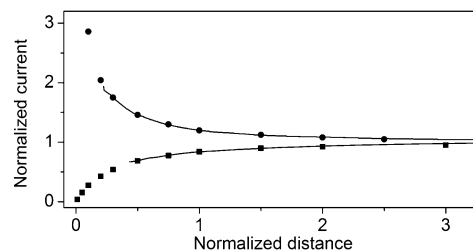
Figure 6. Positive (upper) and negative (lower) experimental feedback approach curves (solid lines) obtained using an insulated SECM pipet probe. The electroactive mediator solution was 5.9 mM $Ru(NH_3)_6^{3+}$ containing 0.5 M KCl as supporting electrolyte. The positive feedback approach curve was obtained upon approaching a 2-mm Pt disk electrode, and the negative feedback approach curve was obtained by approaching a Teflon insulating sheath. Approach curves were obtained using a probe potential of −0.4 V vs Ag/AgCl and a substrate potential of 0 V vs Ag/AgCl (positive approach). The symbols represent positive (●) and negative (■) approach curves for ring electrodes with r_g/b = 1.5.

diffusion coefficient (5.3×10^{-6} cm^2 s^{-1}), C_0 is the bulk concentration of electroactive species, and b is the radius of the disk electrode. Thus, we can calculate a value of b for the ring electrode of 1.6 μm, and this value agrees closely with that estimated using SEM.

Theoretical positive and negative feedback approach curves for ring electrode geometries have been calculated using finite element analysis.[23] Comparison of the theoretical approach curves with experimental data can provide an insight into ring geometry including the a/b ratio and the ratio of the total (including insulating layer) radius to the ring outer radius, r_g/b. Figure 6 shows the experimental positive and negative feedback approach curves (solid lines) obtained for an insulated ring electrode in a solution containing 5.9 mM $Ru(NH_3)_6^{3+}$ and 0.5 M KCl as supporting electrolyte. The normalized distance, L, is the ratio of the ring electrode − substrate distance, d, to the outer radius, i.e., $L = d/b$. Positive feedback approach curves were obtained by approaching a 2-mm Pt disk electrode, and negative feedback approach curves were obtained by approaching Teflon. The approach curves were stopped before an increase of twice the bulk steady-state tip current value ($i_{T,\infty}$) for the conductive substrate and before a decrease to less than 75% of $i_{T,\infty}$ for the insulating substrate, to avoid crashing the tip into the substrate. Due of the fragility of these probes, tip crashes generally cause a complete break of the probe tip. The solid symbols in Figure 6 represent the theoretical approach curves using outer ring radii (b) values of 1.4 (positive feedback) and 1.65 μm (negative feedback). The theoretical responses shown are for ring electrodes with r_g/b and a/b ratios of 1.5 and 0.8, respectively. Therefore, comparison of experimental and theoretical approach curves yields estimated ring electrode radii that are close to those estimated using both SEM analysis and cyclic voltammetry. In particular, the shape of SECM approach curves for ring electrodes is highly sensitive to the outer radius, b.[23] Therefore, the excellent fits obtained using the data shown in Figure 6 indicate that the electrophoretic paint completely retracted from the Au ring during the electrode heating step. Moreover, approach curve analysis has provided an insight into the thickness of the insulating layer around the ring electrode, a parameter that cannot be estimated from cyclic voltammetry analysis.
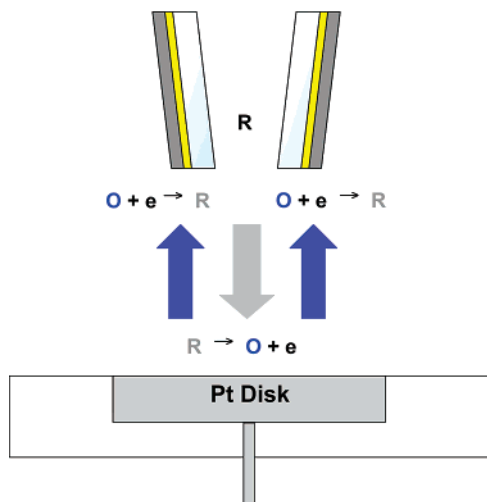
Figure 7. Schematic illustrating the principles of the imaging experiment performed using pipet probes. An electroactive species R is dispensed from the pipet to the substrate, where it is oxidized to O. O then diffuses back to the probe, where it is reduced to R.

Dispensing/Feedback SECM Imaging Experiments. To demonstrate the applicability of these probes in SECM imaging experiments, the oxidation of ferrocenemethanol (FcMeOH) at the substrate was imaged, with simultaneous mapping of the product (FcMeOH$^+$) at the tip. In this experiment, the pipet was filled with a 2 mM FcMeOH/0.5 M KCl solution by applying a vacuum to the pipet while immersed in solution. The electrochemical cell contained 250 μL of 0.5 M KCl (deoxygenated). Dispensing/feedback SECM imaging was performed by applying a constant pressure to the pipet, producing a constant flow of solution, while holding the pipet at a distance of 2.4 μm ($L = 1.5$) from the substrate (a 100-μm-diameter platinum disk embedded in a glass insulating sheath). The amount of solution dispensed from the pipet is a function of the applied pressure, and in typical experiments, the flow rate of solution from the pipet was of the order of 1 nL s^{-1}. Under these conditions, buildup of FcMeOH in the cell solution was sufficiently small to have a negligible effect on the electrochemical measurements. The Pt disk was held at a potential of 0.40 V versus Ag/AgCl to oxidize the dispensed FcMeOH. The pipet probe was held at 0.0 V versus Ag/AgCl to reduce FcMeOH$^+$ that diffused back to the tip. A schematic illustrating this process is shown in Figure 7. The tip was then moved across the Pt disk $x - y$ plane at 300 μm s^{-1} (x long direction). Figure 8 shows the images recorded at the substrate and tip electrodes as the dispensing tip was moved across the Pt substrate. Both i_S and i_T increased as the tip passed over the Pt disk. The i_S and i_T images are not offset to any significant extent in either the x or y direction, indicating that motion of the tip during feedback of electroactive species from the substrate did not affect the apparent location of the platinum substrate, as determined from the tip current image, even at the relatively high scan rates used here. The ability to record good images at relatively high scan rates makes these pipets particularly attractive for rapid screening of large arrays of catalysts, an application that will be described in detail in a future contribution.

The measured tip collection efficiencies, CE_T (i.e., the ratio of the feedback current at the tip to the substrate current) is ~1% This low CE_T value is due to the relative sizes of the tip and
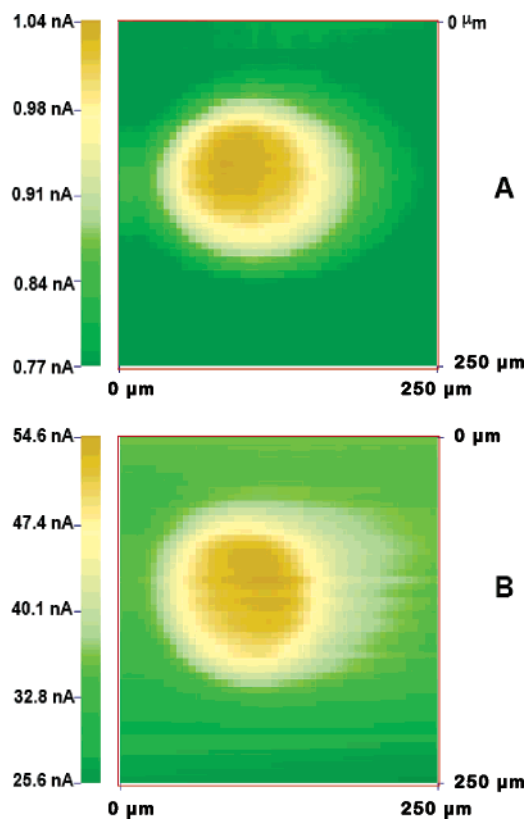

Figure 8. Dispensing/feedback SECM images obtained upon moving an SECM pipet across a 100-μm Pt substrate electrode embedded in glass. The electroactive mediator solution was 2 mM FcMeOH/0.5 M KCl, and the flow rate of solution from the pipet was 1 nL s^{-1}. The pipet—substrate separation was 2.4 μm ($L = 1.5$). The substrate potential was 0.40 V vs Ag/AgCl, and the pipet probe potential was 0.0 V vs Ag/AgCl. The imaging scan rate was 300 μm s^{-1} (x long direction). (A) Image recorded by measuring i_T. (B) Image recorded by measuring i_S.

substrate electrodes. When dispensed from the pipet, FcMeOH was oxidized at the 100-μm substrate electrode, which is a large planar surface when compared to the 3-μm tip. Upon diffusing away from the substrate to the tip, the amount of FcMeOH$^+$ that can be detected is expected to be quite low. However, this small CE_T is not expected to adversely affect the applicability of this technique as extremely small amounts of material and low currents can be detected using the ring electrodes. The solution used in this demonstrative experiment was quite dilute, yet a good image based on i_T (in the subnanoampere range) was obtained. The substrate collection efficiency, CE_S (i.e., the ratio of the amount of material detected electrochemically at the substrate to that dispensed from the pipet), has been found to vary significantly over a large number of experiments and values ranging from 20 to 60% have been recorded. We have attributed this variation to a reduction of the diameter of the pipet aperture by partial blocking with particulate material, causing a decrease in the actual amount dispensed by the pipet. This reduction then causes a decrease in the apparent CE_S value. However, decreased injection volumes may also be attributed to hydrodynamic effects associated with the picoinjector. A series of experiments have also been performed in which low volumes (pL) of solution were dispensed individually from the pipet and transient i_S and i_T responses recorded. These measurements are being pursued to address the issues of CE_S

and CE_T and will also involve detailed calculations involving the flow from the pipet under various conditions, as well as diffusion to each electrode. These measurements and analyses are beyond the scope of this introductory paper and will be addressed in a following contribution. In addition, some novel applications of this SECM approach will be discussed.

CONCLUSIONS

The fabrication and characterization of novel probes for SECM experiments have been described. These probes consist of a hollow, gold-coated micropipet, insulated using electrophoretic paint. Upon curing the electrophoretic paint, the film shrinks slightly, exposing a gold ring electrode. Characterization of these pipet-based SECM probes was performed using SEM and a variety of electrochemical techniques. Using this procedure, routine fabrication of probes with radii of the order of 1.5 μm is possible and this has been confirmed independently by SEM and electrochemical analysis. Positive and negative SECM feedback approach curves obtained using these probes agreed closely with the theoretical responses for ring electrodes with r_g/b and a/b ratios of 1.5 and 0.8, respectively, indicating successful exposure of the ring electrode and the deposition of a relatively thin insulating layer. The application of these probes in SECM imaging experiments was illustrated using a model electroactive species. An SECM image of a 100-μm Pt disk substrate was obtained by dispensing FcMeOH and monitoring the substrate current as the probe passed over the Pt disk. In addition, by monitoring the tip current, it was possible to obtain a map of the oxidation product at the Pt disk as FcMeOH$^+$ diffused away from the disk. This particular ability makes this technique very attractive for catalytic or metabolic screening of materials or microorganisms, respectively, allowing real-time measurement of reaction or metabolic products. Moreover, these probes will be very useful for combined SECM techniques, such as SECM−SCLM, that demand localized injection of reactants. In a following communication, a thorough analysis of the dispensing probe transient response and electrode collection efficiencies will be reported and some novel applications of this new SECM approach will be described.